

The simulation analysis of stator flux droop minimization in direct torque control open-end winding induction machine

Muhammad Zaid Aihsan¹, Auzani Jidin^{2,3}, Siti Azura Ahmad Tarusan^{2,3}, Tole Sutikno^{4,5}

¹Faculty of Electrical Engineering Technology, University Malaysia Perlis, Perlis, Malaysia

²Faculty of Electrical Engineering, Universiti Teknikal Malaysia Melaka, Melaka, Malaysia

³Power Electronics and Drives Research Group, CeRIA, Universiti Teknikal Malaysia Melaka, Melaka, Malaysia

⁴Department of Electrical Engineering, Universitas Ahmad Dahlan, Yogyakarta, Indonesia

⁵Embedded System and Power Electronics Research Group, Yogyakarta, Indonesia

Article Info

Article history:

Received Nov 7, 2022

Revised Jan 8, 2023

Accepted Jan 22, 2023

Keywords:

Direct torque control
Distorted phase current
Induction machine
Open-end winding
Stator flux droop

ABSTRACT

Direct torque control (DTC) using dual-inverter technique is one of the best topologies for electric vehicle (EV) as it offers abundant selection of voltage vectors to drive the induction machine (IM). This dual-inverter technique also more reassuring as the system still workable even any of its voltage supply is disrupted or the power pack is drained. However, during the uneven voltage supply, the movement of voltage vectors is interrupted and will move obliquely especially in medium voltage vectors. This situation will lead to the faulty movement of the voltage vectors in the default sector definitions and lead to huge flux droop, which later could impose to distort phase current. This paper proposes an optimal sector definition based on the preset voltage ratio between the two inverters. The voltage vectors can be mapped tangentially to the flux vector, minimizing the flux droop and improving the phase current waveform when the proposed sector is utilized. The effectiveness of the proposed sector is tested using MATLAB/Simulink software and the exact parameter from the induction machine.

This is an open access article under the [CC BY-SA](https://creativecommons.org/licenses/by-sa/4.0/) license.



Corresponding Author:

Muhammad Zaid Aihsan

Faculty of Electrical Engineering and Technology, Universiti Malaysia Perlis

02600 Arau, Perlis, Malaysia

Email: zaid@unimap.edu.my

1. INTRODUCTION

Induction machines are high-performance motor drives driven by several control techniques, namely vector and scalar control. In vector control, two former known techniques are field oriented control (FOC) and direct torque control (DTC). DTC paid enough attention to this technique due to its fast torque response and simplicity. For the FOC technique, researchers need to know most of the machine parameters and knowledge of the frame transformation, which is more complex than the DTC system. The DTC system only requires stator resistance information and operates by selecting the predefined switching from the look-up table. The first design of DTC [1] has several drawbacks, such as high torque ripple and variable switching frequency due to the usage of a digital hysteresis controller with a low sampling rate. This will allow the delay action, which causes the torque error to struggle to travel within the hysteresis band and easily exceeds the upper band limit (which causes an overshoot condition) or outpace the lower band limit (causing the undershoot phenomenon) [2]–[5]. Next, it will lead to the faulty selection of voltage vector or frequent selection of reverse voltage vector that can cause a steep torque generation [6].

The drawbacks of DTC have been addressed using several methods, with many solutions being suggested. A simple concept known as duty cycle control which employs an active voltage vector for a

portion of the control period and a zero-voltage vector for the remainder is used in research [7]–[10]. This method is easy to be implemented and cost-effective. Investigations on the direct torque control space vector modulation (DTC-SVM) approach were also conducted [11]–[13]. This methodology guarantees the inverter switching frequency remains constant while lowering torque ripple, in addition to the benefits of the DTC approach. Unfortunately, this method is challenging, particularly when solving the reference voltage space vector equation. Another simplest approach is by adjusting the hysteresis band size depicted in [14]–[17] and modifying the size of the hysteresis band to regulate torque precisely. This solution, nevertheless, is suitable for low sampling rate devices like digital signal processor (DSP) controllers and requires a complicated hardware setup. With a minimum sample rate of 50µs for a DTC system using a dSPACE-based controller, there is a chance that the torque will move quickly between the upper and lower band, causing overshoot and undershoot without indication [18]. There has been a lot of interest in a contemporary technique that combines DTC with predictive control because it can lower torque ripple and maintain consistent switching frequency [19]–[21]. To avoid increased torque and flux ripple, this system must properly select the weighting parameters.

Besides different control techniques, many studies on inverter topologies were also covered. Three-level cascaded H-bridge inverters (CHMI) [22], [23] and neutral point clamped multilevel inverters (NPCMI) [24], [25] are examples of multilevel inverter-fed induction machines that have been extensively studied. However, these arrangements need an independent direct current (DC) power source and extra capacitors for voltage balancing, increasing system complexity. Most CHMI and NPCMI use the standard two-level inverter, which can produce two-level voltage inversion by using six active voltage vectors and two null voltage vectors. Meanwhile, the DTC utilizing an open-end windings induction machine (OEWM) can form up to 64 voltages from the multiplication $2^3 \times 2^3$. The combinations of voltage vectors can be categorized as short, medium, or long. This feature enables the DTC system to pick a voltage vector that produces a torque regulation slope with a lower gradient for each torque and speed requirement [26]. Nonetheless, the uneven voltage supply in the dual inverter may cause lower power operation and disturbance at phase current, which later could impose distortion in harmonic current [27], [28]. In addition, voltage vectors travel irregularly and in an oblique direction, especially in medium voltage vectors. Due to this circumstance, the voltage vectors in the default sector definitions will move inaccurately and cause a significant flux droop condition [29]–[31].

With this direction, this paper attempts to solve the issue of stator flux droop in the dual-inverter technique during uneven voltage supply. In the dual inverter, the active voltage vector is formed by the resultant voltage vector between two inverters. The resultant voltage vector created in a balanced voltage supply typically has an angle aligned and tangential to the definitions of the default flux sectors. The angle of the resulting voltage vector yet will be tilted and will not align or be tangential to the default flux sector definitions when the provided voltage is uneven or unbalanced. To address this issue, new flux sector definitions must be developed to satisfy the changing pattern of the voltage vector. The inverters ratio is set to 100:50 for inverter 1 and 100:70 for inverter 2, and the new sector definitions will be designed based on the voltage vectors under this situation. The validity of this research is tested using MATLAB/Simulink using the real motor parameter from De Lorenzo DL 1201. In section 2, the structure of DTC-OEWIM is briefly outlined. Section 3 demonstrate the proposed method using different sector definitions for different voltage ratio. Section 4 demonstrates simulation results and analysis for the conventional and proposed sector definitions. Finally, section 5 provides the findings of this study.

2. THE DIRECT TORQUE CONTROL WITH OPEN-END WINDING CONFIGURATIONS

In order to operate the induction machine in an open-end winding configuration, the normal wye or delta connection is open and breaks into a default three-phase connection and fed to the second inverter. The origin single-sided DTC system from [1] is modified to satisfy the conditions for driving two inverters simultaneously. The (1)–(5) are used to characterize each of the subsystems in the simulation block of the DTC system in terms of space vectors:

$$v_s = r_s i_s + \frac{d\Psi_s}{dt} \quad (1)$$

$$0 = r_r i_r - j\omega_r \Psi_r + \frac{d\Psi_r}{dt} \quad (2)$$

$$\Psi_s = L_s i_s + L_m i_r \quad (3)$$

$$\Psi_r = L_r i_r + L_m i_s \quad (4)$$

$$T_e = \frac{3}{2} P |\Psi_s| |i_s| \sin\delta \tag{5}$$

where ω_r stands for rotor electric angular speed in rad/s, δ indicate angle between the stator flux linkage and the stator current space vectors. P symbolizes the number of pole pairs. The motor inductances represented by L_r , L_s and L_m . From (1), the stator flux of d^s - and q^s - can be expressed as (6) and (7).

$$\Psi_{s,d}^s = \int (v_{s,d}^s - i_{s,d}^s r_s) dt \tag{6}$$

$$\Psi_{s,q}^s = \int (v_{s,q}^s - i_{s,q}^s r_s) dt \tag{7}$$

The phase voltage across the stator winding of the dual inverter can be derived as (8)-(10).

$$V_{AA'} = V_{AN} - V_{A'N'} - V_{NN'} \tag{8}$$

$$V_{BB'} = V_{BN} - V_{B'N'} - V_{NN'} \tag{9}$$

$$V_{CC'} = V_{CN} - V_{C'N'} - V_{NN'} \tag{10}$$

The value of X in $V_{XX'}$ indicates the phase different between phase A, phase B and phase C the phase voltage. The poles voltage of inverter 1, V_{XN} and poles voltage of inverter 2, $V_{X'N'}$ can be measured at inverter leg and ground area.

$$V_{s,d}^s = \frac{V_{dc}}{3} [2 (S_a^{1+} - S_a^{2+}) - (S_b^{1+} - S_b^{2+}) - (S_c^{1+} - S_c^{2+})] \tag{11}$$

$$V_{s,q}^s = \frac{V_{dc}}{\sqrt{3}} [(S_b^{1+} - S_b^{2+}) - (S_c^{1+} - S_c^{2+})] \tag{12}$$

Next, the (6) and (7) can be expressed in terms of switching states S_a^{1+} , S_b^{1+} , S_c^{1+} , S_a^{2+} , S_b^{2+} and S_c^{2+} in a $V_{s,d}^s$ and $V_{s,q}^s$ components of phase voltages. The following is an expression for the switching states above, which are labeled using the binary system method:

$$S_x^{y+/-} = \begin{cases} 1 & \text{Indicates the upper/lower switch is ON} \\ 0 & \text{Indicates the upper/lower switch is OFF} \end{cases} \tag{13}$$

where “+/-” stands for the upper side (+) and lower side (-) of switches in each inverter, and the superscript “y” specifies the number of inverter 1 or inverter 2, as shown in Figure 1.

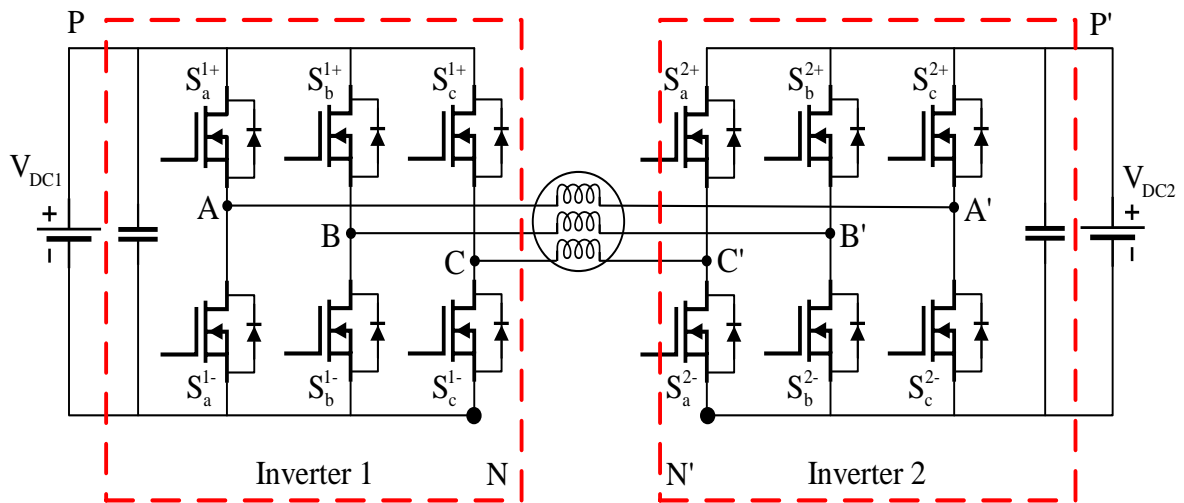


Figure 1. Configuration of open-end winding induction machine supplied using dual-inverters

3. THE UNEVEN DC VOLTAGE SUPPLY

3.1. Problem analysis

In the dual-inverter technique, inverter 1 and inverter 2 are supplied with isolated DC supplies or power packs such as batteries or supercapacitors. From the injected voltage, the voltage vectors form the resultant voltage vector of inverters 1 and 2. By using (11) and (12), the new resultant voltage vector can be found using (13). When the supply voltage is even/equal, the generation of voltage vectors (black arrow) is stable for all types of voltage vectors namely long, medium and short as shown in Figure 2(a), Figure 2(b) and Figure 2(c) respectively. However, when the supply voltage is uneven/unequal, the generation of voltage vectors is affected and tilted as shown in the red arrow. As shown, the long and short voltage vectors reduced magnitude during the uneven voltage vectors. While for medium voltage vectors, the resultant vectors are tilted irregularly and also reduced in magnitude.

Generally, when the voltage vectors deviate in a different direction, or the angle is tilted, it will affect the movement of stator flux in the original sector definition. The default medium voltage vectors have an equal 60° angle forming 6 six sectors. The direction of voltage vectors will no longer be tangential to the flux sector, as portrayed in Figure 3. The vectors are extremely thrust inward or deflected outwards, crossing the hysteresis band limit.

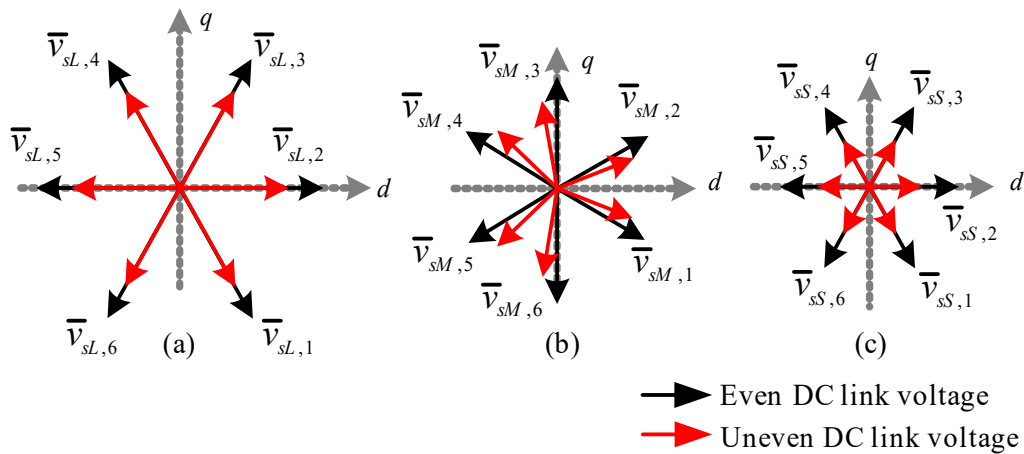


Figure 2. Different between even and uneven DC link voltage in (a) long vectors, (b) medium vectors, and (c) short vectors

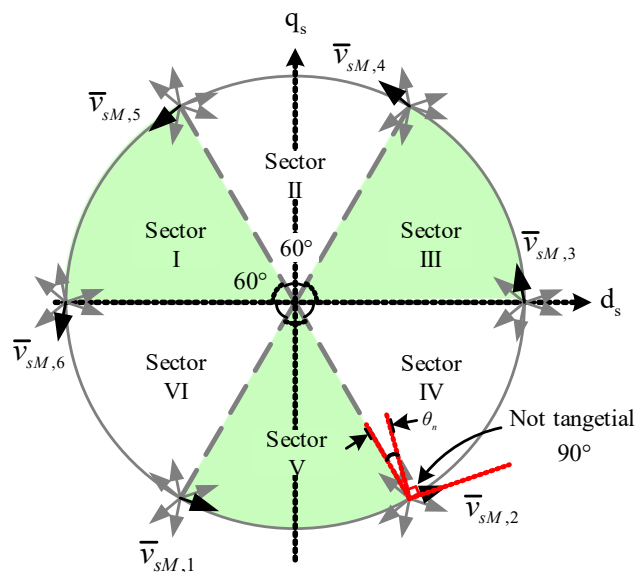


Figure 3. Mapping of new resultant medium voltage vectors to the default sector definition

3.2. New sector design

To counter these issues, the information of deviated voltage vectors for inverter ratio 100:50 and inverter ratio 100:70 is collected for every voltage vector. From there, the new sectors can be designed by ensuring the sector borderline is 90° from the tilted voltage vectors, as shown in Figure 4. Three examples were given where the borderline for $\bar{v}_{sM,1}$, $\bar{v}_{sM,3}$, and $\bar{v}_{sM,5}$ is placed exactly at an 90° angle. It can be observed that the new borderline will be constructed according to the condition of the new voltage vectors.

The new sector detector for an inverter ratio of 10:5 and 10:7 is illustrated in Figures 5(a) and 5(b), respectively. With these sectors, the tilted voltage vectors are now positioned appropriately and tangential to the state of the flux sector. This will allow the movement of the voltage vector in a proper condition, enabling the flux to be regulated in a circular locus. Note that the phase angle for each sector is no longer equal in the new sector. It will vary based on the amount of voltage supplied to both inverters. This is due to the higher the voltage difference between the inverters, the larger the deflected in the voltage vectors.

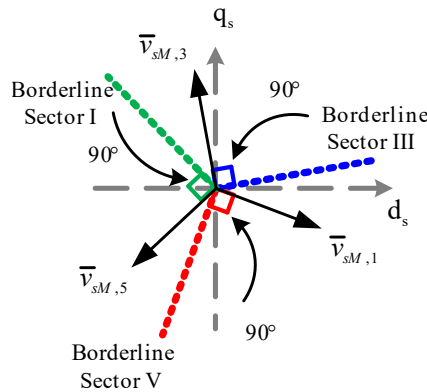


Figure 4. Borderline sector arrangement for new sector definitions

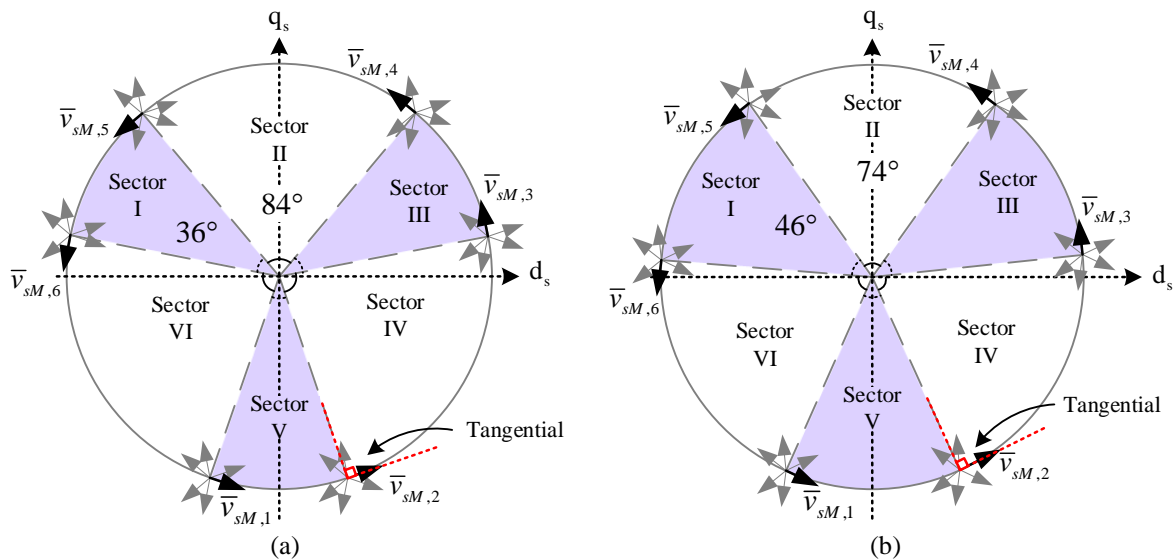


Figure 5. New sector definitions for voltage ratio of (a) 10:5 and (b) 10:7

The new sector (blue box) will be included in the simulation module together with the default sector definition (pink box), as shown in Figure 6. This will allow the DTC system to directly change the sector whenever there is a change in the voltage level in the inverter. The subsystem in Figure 6 comprises a pair of hysteresis comparators for handling the torque and flux controller, torque and flux calculators, a look-up table, a d-q current estimator, an open-end winding induction machine, and a two-unit voltage-source inverters (VSIs).

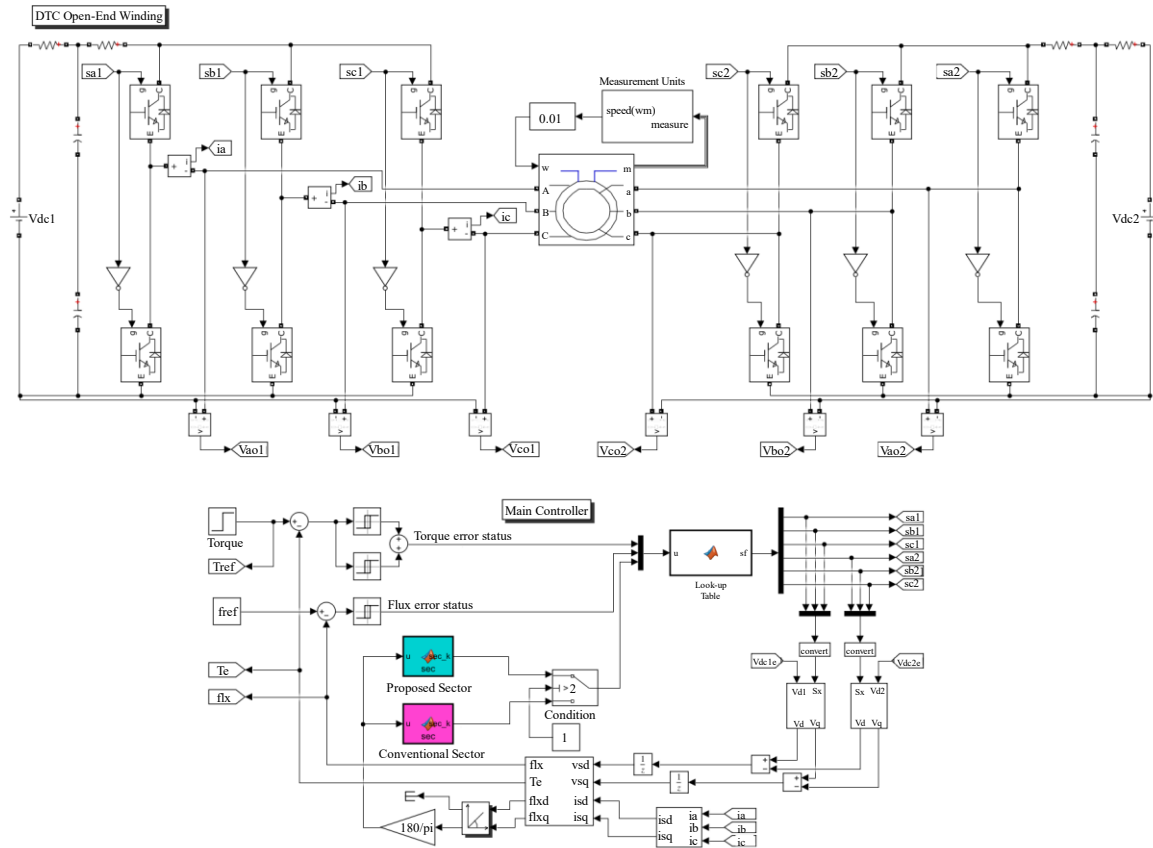


Figure 6. MATLAB Simulink design

4. SIMULATION RESULTS AND ANALYSIS

A simulation is conducted to analyze the proposed sector effectiveness using the exact parameters from the De Lorenzo DL 1021 induction machine as shown in Table 1. The simulation is tested under steady-state operation with different voltage ratios of the inverter. For case 1, the preset ratio is 100:50, and the ratio of 100:70 for case 2. Figure 7(a) shows the default V_d - V_q voltage when both inverters are supplied with 100 V. Constant voltage injection at both sides causes a stable resultant voltage vector to move in the default 60° angle per sector. Nonetheless, when the voltage of any inverter is reduced, the V_d - V_q generation is affected in terms of its magnitude voltage, and the angle for every sector as the resultant voltage vector is now combined from two uneven voltage sources. When the voltage of inverter 2 is reduced to 70 V, and the inverter 1 voltage is maintained to 100 V, the generation of V_d - V_q is affected, as in Figure 7(b). In the same situation when inverter 2 is now reduced to 50 V, the generation of V_d - V_q is more affected, greater reduction in magnitude, and the angle of every sector is tilted even greater, as shown in Figure 7(c).

Table 1. Induction motor parameters

Induction Motor	
Parameter	Value
Rated power, P	1.1 kW
Rated speed, $\omega_{m rated}$	2800 rpm
Stator Resistance, R_s	6.1 Ω
Rotor Resistance, R_r	6.2293 Ω
Mutual Inductance, L_m	0.4634 mH
Rotor self-inductance, L_r	0.47979 mH
Stator self-inductance, L_s	0.47979 mH
Number of pole pairs, p	2

The affected resultant voltage vectors from Figures 7(b) and 7(c) will move in the default sector definitions causing a faulty movement of the flux sector. Figure 8(a) shows the performance of the d-q flux

locus operating under an inverter ratio of 100:50. It shows the movement of the stator flux is not smooth in a circular shape, and there is a segmented curve whenever there is a change between sectors. Fortunately, when the proposed sector for inverter ratio 100:50 is selected, the d-q flux locus improves, as depicted in Figure 8(b). It shows that the locus now is a more circular shape, and the segmented curve for each sector is gone. The same behavior for inverter ratio 100:70 where the movement of stator flux is high in a zig zag pattern is in Figure 9(a), and the d-q flux locus is stated to improve and adequately move in the flux vector as in Figure 9(b).

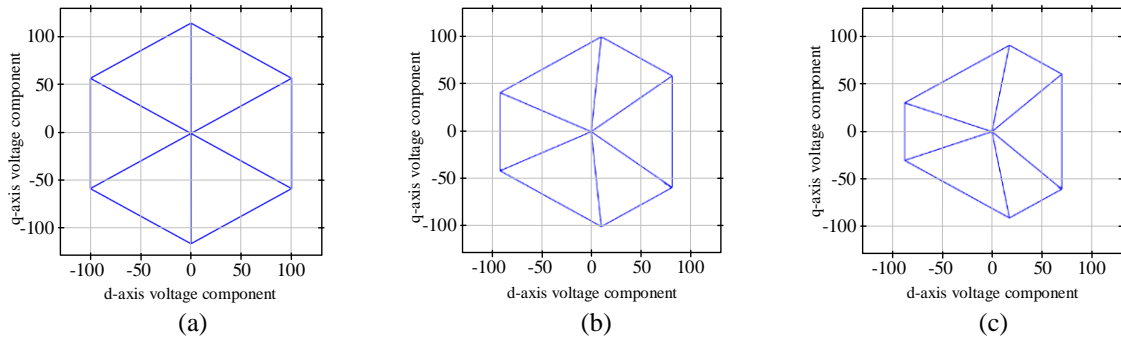


Figure 7. d-q voltage component for inverter ratio (a) 100:100, (b) 100:70, and (c) 100:50

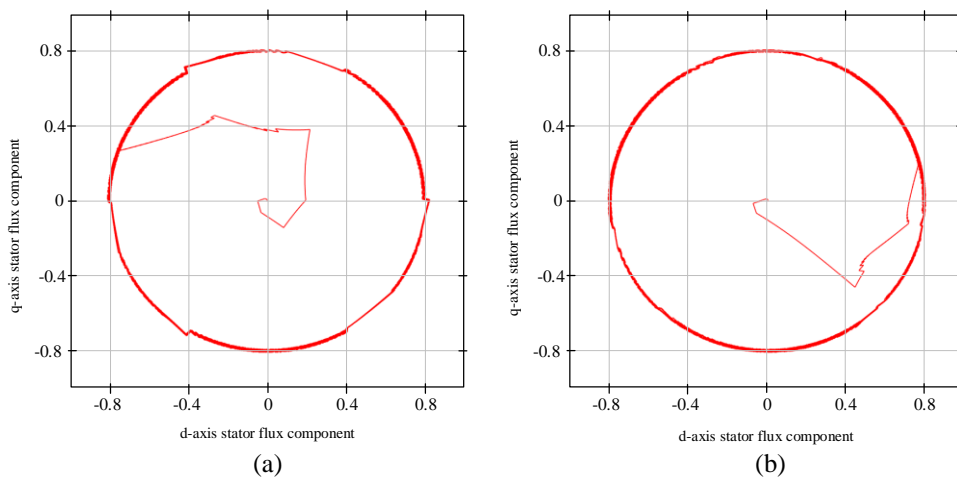


Figure 8. d-q stator flux component locus for inverter ratio 100:50 (a) default sector and (b) proposed sector

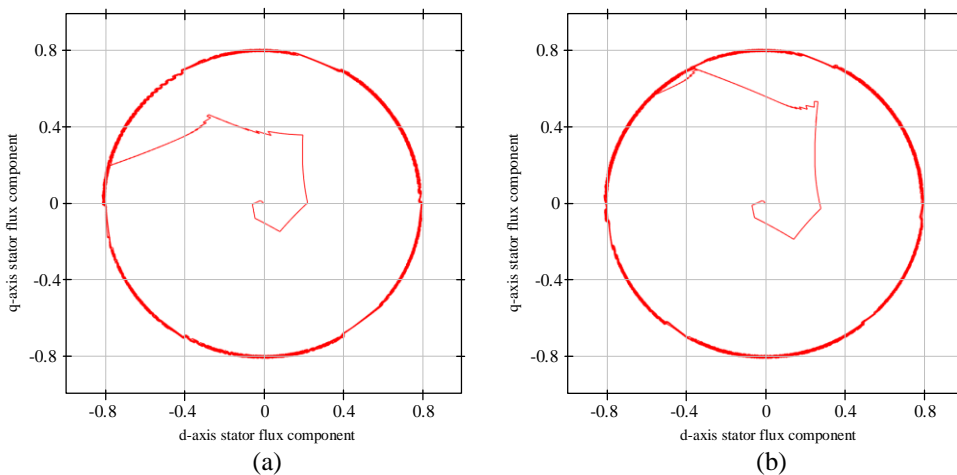


Figure 9. d-q stator flux component locus for inverter ratio 100:70 (a) default sector and (b) proposed sector

Next, the performance of the proposed sector is tested with phase current (upper trace), stator flux magnitude (middle trace), and switching state transitions (bottom trace) for both inverter ratios, as shown in Figures 10 and 11. The performance of stator flux magnitude in the default sector faced a massive flux droop and spike phenomenon. In the default DTC system, the movement of flux in every sector is controlled by two suitable voltage vectors. The term suitable vectors means that the voltage vectors are more tangential to the flux vector. For the uneven voltage supply to the inverter, the generation of resultant vectors is now less tangential in the default sector. Consequently, the voltage vector is unable to increase and decrease the stator flux adequately, thus leading to the droop in stator flux magnitude, especially at the location of the flux changes in its direction between the positive flux locus and negative flux locus. Whenever the proposed sector is enabled, the affected resultant vectors are now moved to the new sector definitions which the vectors are tangential to the flux vector. With this situation, the magnitude of stator flux now improves and reduces the flux droop phenomenon, as shown in Figures 10 and 11 in the proposed sector section.

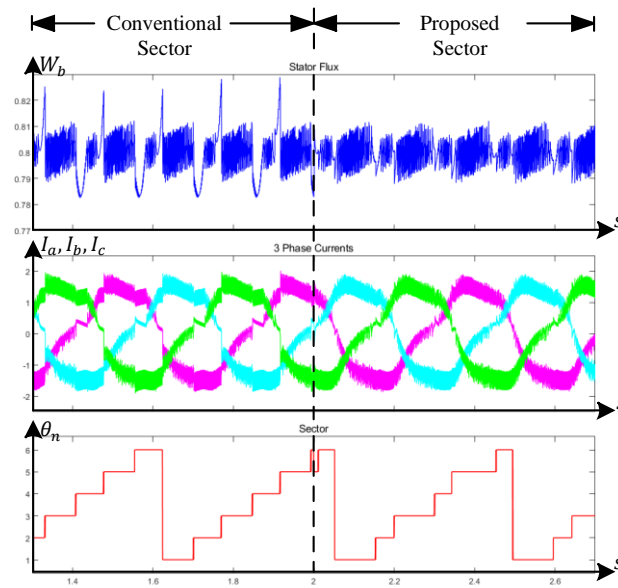


Figure 10. Three-phase current (upper trace), stator flux magnitude (middle trace) and switching state transitions every sector (bottom trace) for inverter ratio 100:50

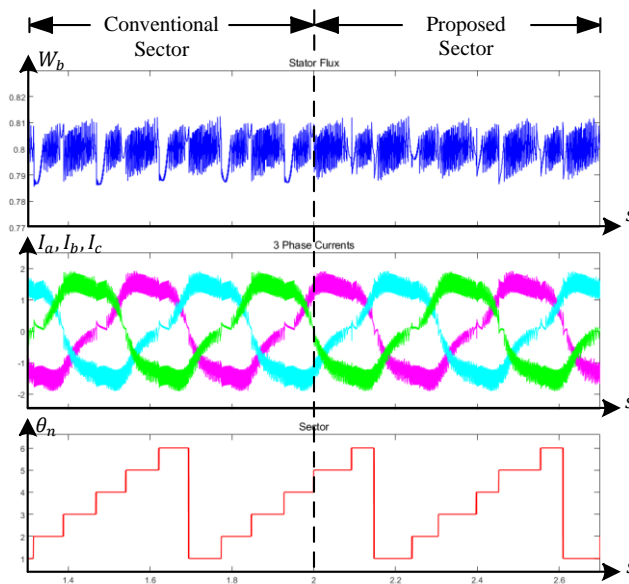


Figure 11. Three-phase current (upper trace), stator flux magnitude (middle trace) and switching state transitions every sector (bottom trace) for inverter ratio 100:70

This flux droop problem will cause another problem in the phase current waveform. Even though the default induction motor current will face a small notching effect at the same location for every cycle, the effect is not critical during the balanced voltage supply. However, when the system operates in an uneven voltage supply, the notching effect becomes more significant, and it appears to have a small current spike at the current magnitude. The notching effect happened at the exact location of the flux droop appears, and this problem is fixed when the proposed sector is flagged ON. The phase current started to improve, with less notching effect during the proposed sector definitions. The bottom trace (red color) is to show the differentiation of sector used between the conventional and the proposed sector definitions.

Another criterion to be analyzed is the d-q current components locus. As shown in Figures 12(a) and 12(b), the current components of i_{sd} and i_{sq} are operated under the default sector definition with the ratio of 100:50 for conventional and proposed sector respectively. Noticeable that the current component locus during uneven voltage supply does not properly regulate and it has 3 areas affected with a wide gap. The gap occurs as a sudden and unexpected movement occurs in the current components of i_{sd} and i_{sq} . This is due to the flux changing to a different sector, but the control vector is not tangential to the flux vector. Fortunately, the current component of i_{sd} and i_{sq} started to regulate and form a good current components locus as in when the proposed sector definitions are used. These current components are important as this information will be multiplied with the flux information to estimate the torque value. A faulty reading will result in poor performance of torque estimation. Figure 13(a) and 13(b) shows the results of current components locus for inverter ratio under 100:70 operation.

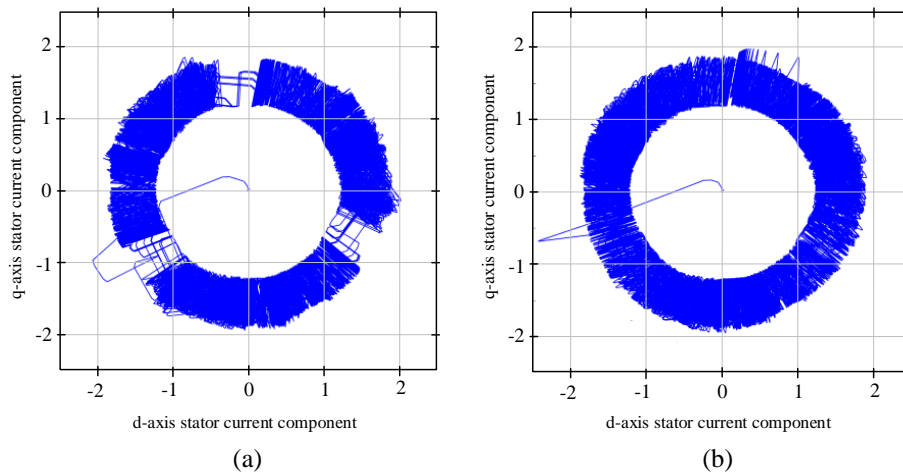


Figure 12. d-q stator current component locus for inverter ratio 100:50 (a) default sector and (b) proposed sector

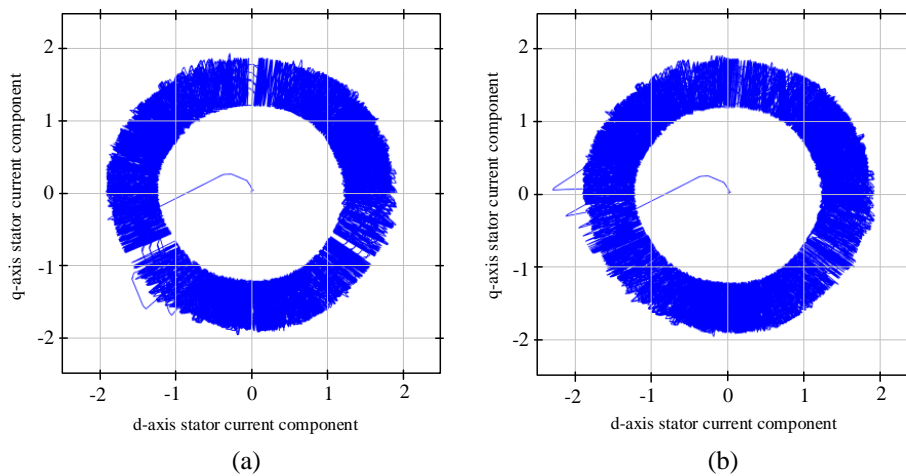


Figure 13. d-q stator current component locus for inverter ratio 100:70 (a) default sector and (b) proposed sector

5. CONCLUSION

A simple approach has been proposed to minimize the stator flux droop in the DTC system for open-end winding configurations, specifically under medium voltage vectors condition. The new sector definitions are promising to cater and retune the movement of voltage vectors tangentially to the flux vector. Thus, it helps to improve the movement of flux and current components, which simultaneously minimizes the stator flux droop situation and improves the phase current performance. This method is simple without complex equations and significantly improves the system.




REFERENCES

- [1] I. Takahashi and T. Noguchi, "A new quick-response and high-efficiency control strategy of an induction motor," *IEEE Transactions on Industry Applications*, vol. IA-22, no. 5, pp. 820–827, Sep. 1986, doi: 10.1109/TIA.1986.4504799.
- [2] A. A. Kadum, "New adaptive hysteresis band width control for direct torque control of induction machine drives," *International Journal of Power Electronics and Drive Systems (IJPEDS)*, vol. 11, no. 4, pp. 1908–1917, Dec. 2020, doi: 10.11591/ijpeds.v11.i4.pp1908-1917.
- [3] M. Zadehbagheri, T. Sutikno, and M. J. Kiani, "A new method of virtual direct torque control of doubly fed induction generator for grid connection," *International Journal of Electrical and Computer Engineering (IJECE)*, vol. 13, no. 1, pp. 1201–1214, Feb. 2023, doi: 10.11591/ijece.v13i1.pp1201-1214.
- [4] Y. Yang, Q. Wang, and J. Shang, "Five-level hysteresis DTC of open-end winding permanent magnet synchronous motors with zero-sequence currents suppression and torque ripple reduction," *IEEE Access*, vol. 10, pp. 121762–121771, 2022, doi: 10.1109/ACCESS.2022.3223126.
- [5] M. Z. Aihsan, A. Jidin, A. Alias, S. A. Ahmad Tarusan, Z. Md Tahir, and T. Sutikno, "Torque ripple minimization in direct torque control at low-speed operation using alternate switching technique," *International Journal of Power Electronics and Drive Systems (IJPEDS)*, vol. 13, no. 1, pp. 631–642, Mar. 2022, doi: 10.11591/ijpeds.v13.i1.pp631-642.
- [6] A. Ajlan, N. R. N. Idris, and S. S. Lee, "Minimization of torque ripple in direct torque control of induction motor at low speed," in *2016 IEEE International Conference on Power and Energy (PECon)*, 2016, pp. 222–227, doi: 10.1109/PECON.2016.7951563.
- [7] M. R. Nikzad, B. Asaei, and S. O. Ahmadi, "Discrete duty-cycle-control method for direct torque control of induction motor drives with model predictive solution," *IEEE Transactions on Power Electronics*, vol. 33, no. 3, pp. 2317–2329, Mar. 2018, doi: 10.1109/TPEL.2017.2690304.
- [8] H. Sudheer, S. F. Kodad, and B. Sarvesh, "Improvements in direct torque control of induction motor for wide range of speed operation using fuzzy logic," *Journal of Electrical Systems and Information Technology*, vol. 5, no. 3, pp. 813–828, Dec. 2018, doi: 10.1016/j.jesit.2016.12.015.
- [9] S. A. Ahmad Tarusan, A. Jidin, M. L. Mohd Jamil, K. Abdul Karim, and T. Sutikno, "A review of direct torque control development in various multilevel inverter applications," *International Journal of Power Electronics and Drive Systems (IJPEDS)*, vol. 11, no. 3, pp. 1675–1688, Sep. 2020, doi: 10.11591/ijpeds.v11.i3.pp1675-1688.
- [10] F. Niu *et al.*, "A simple and practical duty cycle modulated direct torque control for permanent magnet synchronous motors," *IEEE Transactions on Power Electronics*, vol. 34, no. 2, pp. 1572–1579, Feb. 2019, doi: 10.1109/TPEL.2018.2833488.
- [11] S. Massoum, A. Meroufel, A. Massoum, and W. Patrice, "DTC based on SVM for induction motor sensorless drive with fuzzy sliding mode speed controller," *International Journal of Electrical and Computer Engineering (IJECE)*, vol. 11, no. 1, pp. 171–181, Feb. 2021, doi: 10.11591/ijece.v11i1.pp171-181.
- [12] X. Wang, Z. Wang, M. Cheng, and Y. Hu, "Remedial strategies of T-NPC three-level asymmetric six-phase PMSM drives based on SVM-DTC," *IEEE Transactions on Industrial Electronics*, vol. 64, no. 9, pp. 6841–6853, Sep. 2017, doi: 10.1109/TIE.2017.2682796.
- [13] I. Rkik, M. El Khayat, A. Ed-Dahhak, M. Guerbaoui, and A. Lachhab, "An enhanced control strategy based imaginary swapping instant for induction motor drives," *International Journal of Electrical and Computer Engineering (IJECE)*, vol. 12, no. 2, pp. 1102–1112, Apr. 2022, doi: 10.11591/ijece.v12i2.pp1102-1112.
- [14] I. M. Alsofyani, N. R. N. Idris, and K.-B. Lee, "Dynamic hysteresis torque band for improving the performance of lookup-table-based DTC of induction machines," *IEEE Transactions on Power Electronics*, vol. 33, no. 9, pp. 7959–7970, Sep. 2018, doi: 10.1109/TPEL.2017.2773129.
- [15] I. M. Alsofyani and K.-B. Lee, "Evaluation of direct torque control with a constant-frequency torque regulator under various discrete interleaving carriers," *Electronics*, vol. 8, no. 7, Jul. 2019, doi: 10.3390/electronics8070820.
- [16] S. S. Hakami and K.-B. Lee, "Four-level hysteresis-based DTC for torque capability improvement of IPMSM fed by three-level NPC inverter," *Electronics*, vol. 9, no. 10, Sep. 2020, doi: 10.3390/electronics9101558.
- [17] P. S. Borse, M. P. Thakre, and R. Shrivastava, "Employment of torque-hysteresis controller for DTC based induction motor drive," *Journal of Physics: Conference Series*, vol. 2062, no. 1, Nov. 2021, doi: 10.1088/1742-6596/2062/1/012020.
- [18] N. El Ouanjli *et al.*, "Real-time implementation in dSPACE of DTC-backstepping for a doubly fed induction motor," *The European Physical Journal Plus*, vol. 134, no. 11, Nov. 2019, doi: 10.1140/epjp/i2019-12961-x.
- [19] K. Kakouche *et al.*, "Model predictive direct torque control and fuzzy logic energy management for multi power source electric vehicles," *Sensors*, vol. 22, no. 15, Jul. 2022, doi: 10.3390/s22155669.
- [20] A. Berzoy, J. Rengifo, and O. Mohammed, "Fuzzy predictive DTC of induction machines with reduced torque ripple and high-performance operation," *IEEE Transactions on Power Electronics*, vol. 33, no. 3, pp. 2580–2587, Mar. 2018, doi: 10.1109/TPEL.2017.2690405.
- [21] P. Karlovsky and J. Lettl, "Induction motor drive direct torque control and predictive torque control comparison based on switching pattern analysis," *Energies*, vol. 11, no. 7, Jul. 2018, doi: 10.3390/en11071793.
- [22] P. Naganathan and S. Srinivas, "Direct torque control techniques of three-level h-bridge inverter fed induction motor for torque ripple reduction at low speed operations," *IEEE Transactions on Industrial Electronics*, vol. 67, no. 10, pp. 8262–8270, Oct. 2020, doi: 10.1109/TIE.2019.2950840.
- [23] F. Khoucha, M. S. Lagoun, A. Kheloui, and M. El Hachemi Benbouzid, "A comparison of symmetrical and asymmetrical three-phase H-bridge multilevel inverter for DTC induction motor drives," *IEEE Transactions on Energy Conversion*, vol. 26, no. 1, pp. 64–72, Mar. 2011, doi: 10.1109/TEC.2010.2077296.
- [24] P. Li, L. Zhang, B. Ouyang, and Y. Liu, "Nonlinear effects of three-level neutral-point clamped inverter on speed sensorless




- control of induction motor,” *Electronics*, vol. 8, no. 4, Apr. 2019, doi: 10.3390/electronics8040402.
- [25] Z. M. Tahir, A. Jidin, and M. L. M. Jamil, “Multi-carrier switching strategy for high-bandwidth potential balancing control of multilevel inverters,” *International Journal of Power Electronics and Drive Systems (IJPEDS)*, vol. 12, no. 4, pp. 2384–2392, Dec. 2021, doi: 10.11591/ijped.v12.i4.pp2384-2392.
- [26] B. Farid, B. Tarek, and B. Sebti, “Fuzzy super twisting algorithm dual direct torque control of doubly fed induction machine,” *International Journal of Electrical and Computer Engineering (IJECE)*, vol. 11, no. 5, pp. 3782–3790, Oct. 2021, doi: 10.11591/ijece.v11i5.pp3782-3790.
- [27] J. Wei, X. Kong, W. Tao, Z. Zhang, and B. Zhou, “The torque ripple optimization of open-winding permanent magnet synchronous motor with direct torque control strategy over a wide bus voltage ratio range,” *IEEE Transactions on Power Electronics*, vol. 37, no. 6, pp. 7156–7168, Jun. 2022, doi: 10.1109/TPEL.2022.3146155.
- [28] Y. Luo and C. Liu, “A simplified model predictive control for a dual three-phase PMSM with reduced harmonic currents,” *IEEE Transactions on Industrial Electronics*, vol. 65, no. 11, pp. 9079–9089, Nov. 2018, doi: 10.1109/TIE.2018.2814013.
- [29] R. E. Kodumur Meesala and V. K. Thippiripati, “An improved direct torque control of three-level dual inverter fed open-ended winding induction motor drive based on modified look-up table,” *IEEE Transactions on Power Electronics*, vol. 35, no. 4, pp. 3906–3917, Apr. 2020, doi: 10.1109/TPEL.2019.2937684.
- [30] W. S. H. Wong and D. Holliday, “Minimisation of flux droop in direct torque controlled induction motor drives,” *IEE Proceedings-Electric Power Applications*, vol. 151, no. 6, 2004, doi: 10.1049/ip-epa:20040681.
- [31] I. M. Alsofyani, Y. Bak, and K.-B. Lee, “Fast torque control and minimized sector-flux droop for constant frequency torque controller based DTC of induction machines,” *IEEE Transactions on Power Electronics*, vol. 34, no. 12, pp. 12141–12153, Dec. 2019, doi: 10.1109/TPEL.2019.2908631.

BIOGRAPHIES OF AUTHORS






Muhammad Zaid Aihсан    received the B.Eng. and M.Sc. degrees in Electrical Engineering from Universiti Malaysia Perlis, Malaysia, in 2013 and 2016, respectively. He is currently working on the Ph.D. degree under Power Electronics and Drives Research Group (PEDG) in the Faculty of Electrical Engineering, Universiti Teknikal Malaysia Melaka (UTeM), Malaysia. He is a Lecturer at Universiti Malaysia Perlis (UniMAP), Malaysia. His research interests include the power electronics and motor drive systems. He can be contacted at email: zaid@unimap.edu.my






Auzani Jidin    received the B.Eng. degrees, M.Eng. degrees and Ph.D. degree in power electronics and drives from Universiti Teknologi Malaysia, Johor Bahru, Malaysia, in 2002, 2004 and 2011, respectively. He is currently an academician in Faculty of Electrical Engineering, Universiti Teknikal Malaysia Melaka, Melaka, Malaysia. He is also an active researcher in Power Electronics and Drives Research Group (PEDG) that established under the same faculty. His research interests include power electronics, motor drive systems, field-programmable gate array, and DSP applications. He can be contacted at email: auzani@utem.edu.my



Siti Azura Ahmad Tarusan    received the B.Eng. degrees from Universiti Teknologi Malaysia, Johor Bahru, Malaysia, in 2008 and M.Eng. degrees from Universiti Malaya, Malaysia, in 2012. She is currently an academician in Faculty of Electrical Engineering, Universiti Teknikal Malaysia Melaka, Melaka, Malaysia. She is also an active researcher in Power Electronics and Drives Research Group (PEDG) that established under the same faculty. Her research interests include power electronics and motor drive systems. She can be contacted at email: sitiadura@utem.edu.my



Tole Sutikno    is a Lecturer in Electrical Engineering Department at the Universitas Ahmad Dahlan (UAD), Yogyakarta, Indonesia. He received his B.Eng., M.Eng. and Ph.D. degree in Electrical Engineering from Universitas Diponegoro (Semarang, Indonesia), Universitas Gadjah Mada (Yogyakarta, Indonesia) and Universiti Teknologi Malaysia (Johor, Malaysia), in 1999, 2004 and 2016, respectively. He has been an Associate Professor in UAD, Yogyakarta, Indonesia since 2008. He is currently an Editor-in-Chief of the TELKOMNIKA, Director of LPPi UAD, and the Head of the Embedded Systems and Power Electronics Research Group. His research interests include the field of digital design, industrial electronics, industrial informatics, power electronics, motor drives, industrial applications, FPGA applications, artificial intelligence, intelligent control, embedded system and digital library. He can be contacted at email: tole@ee.uad.ac.id.